TELKOMNIKA Indonesian Journal of Electrical Engineering
Vol.12, No.1, January 2014, pp. 388 ~ 397
DOI: http://dx.doi.org/10.11591/telkomnika.v12i1.4142

Research on Space Target Recognition Algorithm Based on Empirical Mode Decomposition

Xia Tian, Hou Chengyu*, and Shen Yiying
School of Electronics and Information Engineering
Harbin Institute of Technology, Harbin, 150001, PR China
*Corresponding author, e-mail: houcy@hit.edu.cn

Abstract

The space target recognition algorithm, which is based on the time series of radar cross section (RCS), is proposed in this paper to solve the problems of space target recognition in the active radar system. In the algorithm, EMD method is applied for the first time to extract the eigen of RCS time series. The normalized instantaneous frequencies of high-frequency intrinsic mode functions obtained by EMD are used as the eigen values for the recognition, and an effective target recognition criterion is established. The effectiveness and the stability of the algorithm are verified by both simulation data and real data. In addition, the algorithm could reduce the estimation bias of RCS caused by inaccurate evaluation, and it is of great significance in promoting the target recognition ability of narrow-band radar in practice.

Keywords*: time series of RCS, empirical mode decomposition, target recognition*

1. Introduction

Radar cross section (RCS) is the available information for almost all types of eigen instrumentation radars. How to make the best use of the space target's RCS information is very important to promote the target recognition ability of narrow-band radar commissioned [1]. RCS is correlated with many factors, such as the target conformation and structure, the target attitude, radar observation angle and external environment, etc. A small fluctuation in these factors changes RCS greatly. For example, a tiny change in the attitude of a high-frequency target would cause a change in RCS of dozens decibels, and the complicated environment in practice would lead to the extremely complex changes in RCS. These would make the calculation of the target structure information from the target RCS more difficult. Therefore, how to use the RCS information is a big problem in the field of radar target recognition [2].

Nowadays using the target RCS information to recognize the target could be achieved by the target RCS time series. When the ground radar stays motionless and the target flies along a definite track, the changes of the target motion track and its attitude are continuous, and a function in which the target echo intensity fluctuates over time is formed. According to radar equation, the echo intensity sequence could be transformed into RCS sequence. Because the space target RCS time series include plenty of information, its existing eigen could be used to recognize the new target, which is the main research content of this paper.

Two kinds of methods are often used to extract the eigen of RCS time series. One is the traditional statistical analytical method. As in Ref. 3, a power spectral density function is applied to observe RCS time series, but it fails to extract recognition index for its insufficient recognizable ability. In Ref. 4, a fighter and a helicopter are taken as the targets, multiple distribution models, such as, χ^2 distribution and lognormal distribution are applied to study the statistical distribution characterization of the RCS time series, but it needs numerous samples to verify. In Ref. 5 the method of analyzing time series with ARMA model is applied to extract the precession period of ballistic target, because RCS time series of the moving space target is often non-stationary time series, it is very difficult to be extracted and recognized by the conventional time series [6, 7] analysis. Therefore, the other one, i.e. non-stationary signal analytical method, is adopted by many scholars now. Fractional Brownian motion model is introduced in Ref. 8 to analyze the RCS time series. The present research is mainly based on the application of wavelet transform and fuzzy classification to extract the eigen and recognize the space target [9-12]. However, the wavelet analysis possesses a poor time resolution in the

Received June 25, 2013; Revised August 26, 2013; Accepted September 19, 2013

low frequency part and a poor frequency resolution in the high frequency part. Furthermore, it depends on the selection of wavelet function, which limits its application. In order to search for the good nature of time-frequency localization, a new method for analyzing the time-frequency of nonlinear, non-stationary signal, i.e. Hilbert-Huang Transform (HHT), was proposed by Norden E. Huang et al in 1996 [13], modified in 1999 [14]. HHT is proved to possess all advantages of the wavelet analysis, and its spectral structure is more accurate. Moreover, the results with clear physical meaning could be obtained directly from spatial domain. Since the EMD, the very core of HHT, was proposed, it has been highly concerned by domestic and overseas scholars specializing in such fields as atmospheric sciences, physical oceanography, remote sensing, mechanical engineering and life sciences, etc. The method has been widely used in such aspects as fault diagnostic testing, noise silencing and multi-scale separation. For example, the method is applied by Loutridis et al to test the fault of machine rotor and excellent performance is achieved [15]. The EMD method is proved to possess excellent filter properties by Flandrin [16]. It is also used by Lin Zhenshan et al to analyze the temperature changes in the northern hemisphere over the past 400 years and results in that climate temperature changes regularly in different time scale [17]. In this paper, EMD analysis would be performed on RCS time series to explore the effective method to extract the eigen.

2. Introduction to EMD Principle

HHT is composed of EMD and Hilbert Transform. In HHT every signal are assumed to be composed of several Intrinsic Mode Functions (IMF), in which IMF should meet two conditions below:
Within the entire time course, the number of crossing zero is equivalent to the number of the extreme points or differs by one at most.
Any point on the signal, the means of both the upper envelope and the lower envelope are zero, namely, the signals are locally symmetrical along the time axis.

The EMD approach was proposed by Huang et al to resolve any given signals. This is a kind of experience sieving method. Its process is described below:
As for any given signal $X(t)$, all of the extreme points on $X(t)$ are identified at first, and then quadratic spline curve is performed on them to connect all points of maximum values to form the upper envelope, and the lower envelope is developed by the same way. The difference of the data $X(t)$ and the means m_1 of the upper and the lower envelopes is recorded as h_1, then it shows as follows:

$$h_1 = X(t) - m_1 \tag{1}$$

The residual signal r_1 including the elements of the lower order frequency is given in the following formula:

$$r_1 = X(t) - h_1 \tag{2}$$

r_1 is taken as the new signal. The above sieving steps are repeated on it, until the residual signal of the nth order becomes monotonic function and fails to sieve IMF components.

$$r_n = r_{n-1} - h_n \tag{3}$$

Mathematically, $X(t)$ could be expressed as the sum of N components of IMF and one residual item:

$$X(t) = \sum_{j=1}^{N} h_j(t) + r_n(t) \tag{4}$$

3. Target Recognition Algorithm Based on EMD

As shown in (4), any signal could be decomposed into a sum of N IMFs and one residual item. As for IMF i, m_i which represents the number of crossing zero could be calculated, and its normalized instantaneous frequency F_i is defined in the paper to be the ratio of its numbers of crossing zero to the length H of the time series, which is expressed as:

$$F_i = m_i / H \quad , i = 1, 2, 3, \cdots, N \tag{5}$$

The energy ratio E_i of IMF i is defined as the percentage of the energy e_i on the total sum of each IMF energy, its expression is as follows:

$$E_i = e_i / \sum_{j=1}^{n} e_j \times 100\% \quad , i = 1, 2, 3, \cdots, N \tag{6}$$

The properties of the target RCS frequency could be often divided into two parts, the rapidly varying part and the slow one. The latter is determined by the influences of observation angle and measurement errors, etc., while the former is related to the changes in the target's conformation, structure and attitude. Taken the actual high-frequency target as an example, the energies of the reflected signals from the nose and the wing of a plane are in great difference, a tiny change in the target attitude could cause a variance in irradiation area and make RCS change by dozens decibels, thus it is seen that the high frequency part of RCS time series represents mainly the properties of the target. Accordingly, if two RCS time series are the same target, their normalized instantaneous frequencies (defined as F_i and F'_i respectively) obtained by EMD should be similar on the high frequency. Based on this characteristic, frequency threshold D is set in this paper to be the division between high frequency and low frequency of IMFs. IMFs are arranged in descending order of the instantaneous frequencies, and they are recorded as $\mathrm{IMF1}, \mathrm{IMF2}, \cdots, \mathrm{IMF}N$. If there is

$$F_j \geq D \quad , j = 1, 2, 3, \cdots, N \tag{7}$$

IMF j would be initially selected for recognition. It is assumed that there are M high frequencies and their IMF meets (7). In order to reduce the negative effects of high-frequency noises, the energy threshold is set as G, if there is

$$E_j \geq G \quad , j = 1, 2, 3, \cdots, M \tag{8}$$

IMF j would be selected as the parameter for recognition, otherwise it would be excluded. Suppose if K IMFs meet the requirements and their instantaneous frequencies are taken as the eigen frequencies for recognition, the recognition index R would be defined as follows：

$$R_j = (F_j - F_{j'}) / F_{j'} \times 100\% \leq \lambda, \quad , j = 1, 2, 3, \cdots K. \tag{9}$$

λ is recognition threshold, which should be often the positive number less than 0.5. If the above formula is met, then there is $S_i = 1$, otherwise $S_i = 0$. Therefore, the total recognition coefficient S is shown as follows:

$$S = \sum_{i=1}^{K} S_k \geq K / 2 \tag{10}$$

If S is greater than or equal to $K/2$, they would be identified to be the same target, otherwise the different targets. Figure 1 is the flowchart of the algorithm presented by this paper.

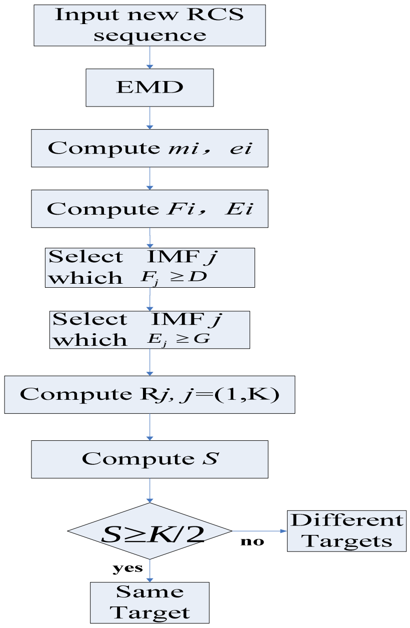

Figure 1. The flowchart of the algorithm presented by this paper

4.The Analysis of Simulated Data

At first, simulated data would be used to verify the effectiveness and the stability of the algorithm presented by this paper. Shown as Figure 2, RCS Sequence 1 is the curve of a RCS value, which changes with time, calculated by radar RCS fluctuation statistical model formula, described as Ref. 3. Suppose if there is a fixed radar station on a certain ground and its working wavelength is 5cm, a jet levels off in the direction of the radar at 30km away from it, the flight height is 3km, the flight speed is 0.5km/s. The sequence length is 212 points and the spent time is 32.12 seconds.

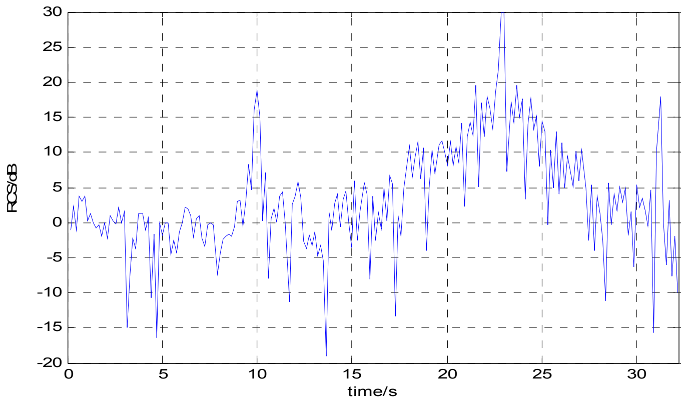

Figure 2. RCS Sequence 1

EMD is performed on the RCS time series and obtained data is shown as Figure 3. The line at the bottom is its envelope information, and IMFs are listed in descending order of the normalized instantaneous frequencies. The energy percentage of the normalized instantaneous frequencies of each IMF is shown as Table 1.

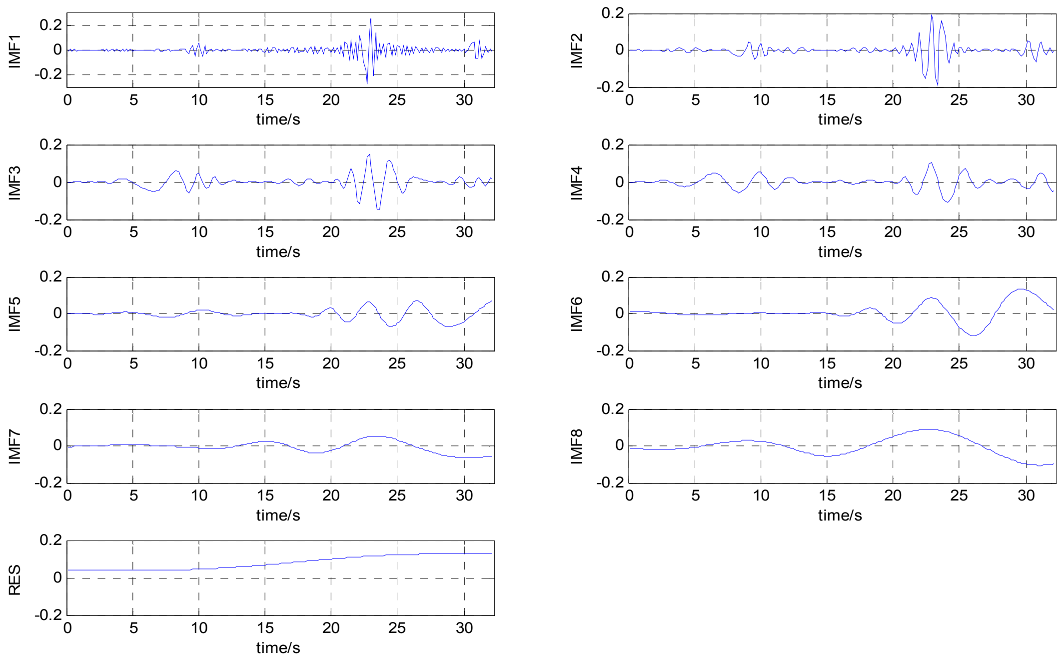

Figure 3. EMD of RCS Sequence 1

Table 1. Normalized instantaneous frequencies and energy ratios of Sequence 1 and 2

IMF	1	2	3	4	5	6	7	8
Instantaneous frequency of Sequence 1	0.7 453	0.3 821	0.2 028	0.1 415	0.0 755	0.0 472	0.0 283	0.0 189
Instantaneous frequency of Sequence 2	0.7 547	0.3 538	0.1 981	0.1 085	0.0 472	0.0 283	No ne	No ne
IMF energy ratio(%) of Sequence 1	16. 14	11. 05	10. 71	7.9 9	6.7 5	20. 00	6.9 2	20. 45
IMF energy ratio(%) of Sequence 2	23. 45	5.3 9	2.9 9	1.1 6	12. 02	54. 98	No ne	No ne

The stability of this algorithm would be analyzed below, it would be considered from two aspects, the presence of measurement error and observation time error.

1) Considering the presence of measurement error

Even if it is the highly accurate radar equipment, the set of sampled data always includes 1%~2%, sometimes even as much as 10%~20% (for example, when the high elevation tracking is performed by radar) of the data which deviate severely from the target true value because of the comprehensive influences or effects of manifold occasional factors [18]. Hence, the extreme value of the data is sometimes caused by measurement error, but not by the real extreme point of the data. In order to verify the stability of the algorithm, suppose if maximum and minimum values have errors in measurement, five maximum values and five minimum values would be excluded and would be replaced with their means of two neighboring points. The reformed RCS Sequence is recorded as Sequence 2, as shown in Figure 4.

EMD is performed on the RCS time series, and the normalized instantaneous frequencies of each IMF and the energy percentage are shown as Table 1. It is found that the numbers of IMF of RCS Sequence 1 and 2 obtained by EMD are different and two IMFs are missing, in the paper the frequency threshold *D* is taken as 0.1, the energy threshold *G* is 5%, the recognition threshold λ is 10% (which is applied to all data below and would not be repeated later). By calculation four IMFs in Sequence 2 are identified to be the high-frequency IMF, but the energies of IMF3 and IMF4 are less than the energy threshold, they could be regarded as high-frequency noises and would be excluded. Sequence 2 relative to the recognition index of Sequence 1 R_1=1.26%, R_2=7.41% are both less than the recognition threshold λ, S=2. When S is more than or equal to the half of the recognition index amount (K/2=1), they could be determined to be the same target. Therefore, the algorithm can still work when the sequences have abnormal values caused by some measurement errors.

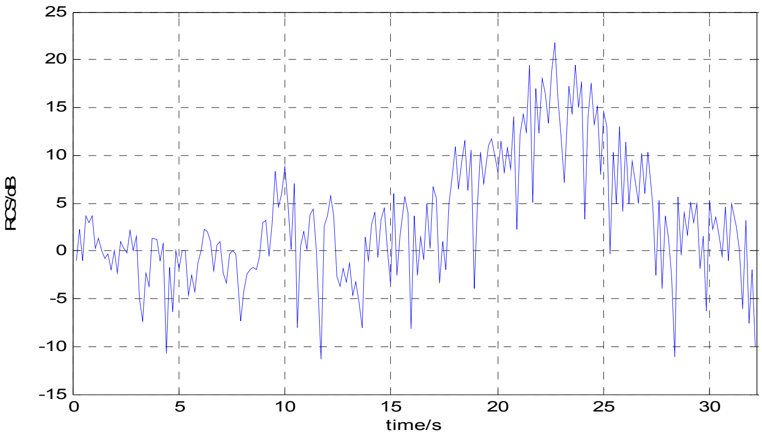

Figure 4. RCS Sequence 2 after the abnormal values are excluded

5. Considering the Presence of Observation Time Error

In order to ensure the successful completion of some tasks, flight vehicles in the military field are required to approach the target in the definite direction or direction interval to maximize the reduction of RCS and to conceal themselves. In the civil aviation system, the leg which is expected to be passed in the flight plan is pre-planned and every leg is a directed flight, so the track line of the space target possesses certain predictability. However, the current RCS time series obtained by observation and the previous ones have a certain error in time because of a tiny change in radar observation time or in the space target attitude. Considering that the algorithm should possess a definite stability in the time, the middle section from 51 to 150 points is cut off from the sequence with the total length of 212 points and is used as the reference sequence, recorded as Sequence 3. Compare it with Sequence 4 which is translational over time, then the results are shown as Figure 5. For example, if Sequence 4 makes the translation motion by 10 points rightwards relative to Sequence 3, it makes the translational motion by 10% relative to the original sequence.

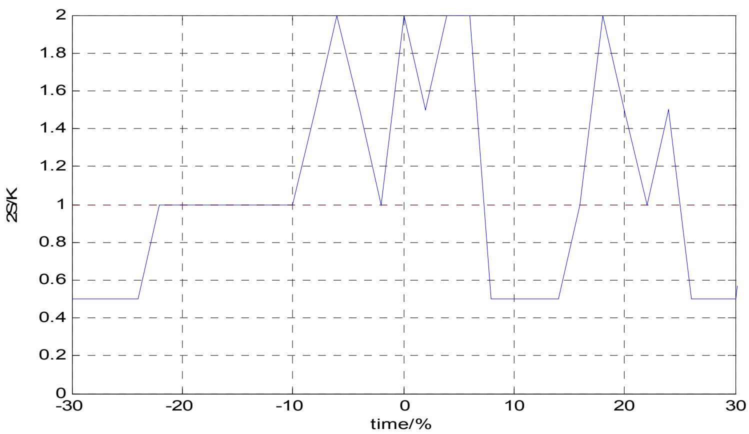

Figure 5. The recognition results of Sequence 4 relative to Sequence 3

The ratio $2S/K$ of the total recognition coefficients of Sequence 4 relative to Sequence 3 to its total recognition threshold K/2 is calculated to change with time, shown as the solid line in Figure 5. If there is $2S/K \geq 1$, the same target would be determined, so it is the correct recognition when the solid line is above the dash line. Seen from the above figure, the recognition effects of this algorithm is comparatively stable when the overlapping time of these two sequences is more than 75% of the total length of the sequences, except for the data whose time translation are between 8% and 16%.

6. The Analysis of the Data from the Real Test

The effectiveness and stability of the algorithm presented here would be verified by a group of data from the real test in the following. In the actual flight, the high end of the fluctuant time spectrum of the airplane's RCS would be much higher. What is shown as Figure 6 is the RCS time series in real test, recorded as Sequence 5, given additionally by Ref. 3, its length is 217 points and the total time is 2.58 seconds.

Considering that the algorithm should possess a definite stability in the time, the middle section from 51 to 150 points is cut off from Sequence 5 with the total length of 217 points and is used as the reference sequence, which is recorded as Sequence 6. Compare it with Sequence 7 which is translational over time, and the results are shown as Figure 7. Seen from the figure, the longer the overlapping time of these two sequences, which is greater than 70% of the sequence's total length, the better the similarity, the more stable the algorithm. Therefore, this algorithm could be concluded to possess a definite stability by the verification of the simulated data and the real data.

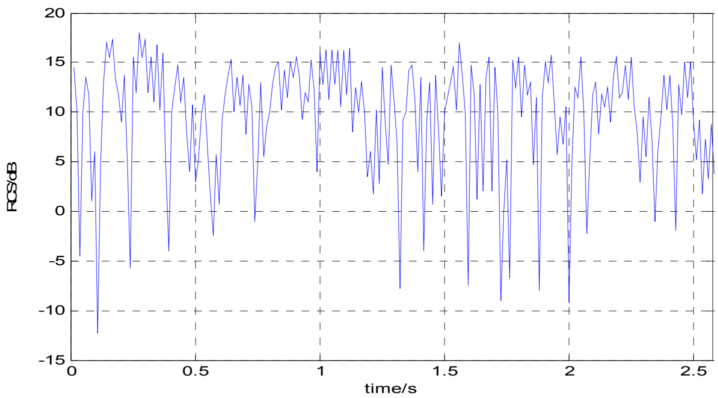

Figure 6. RCS Sequence 5

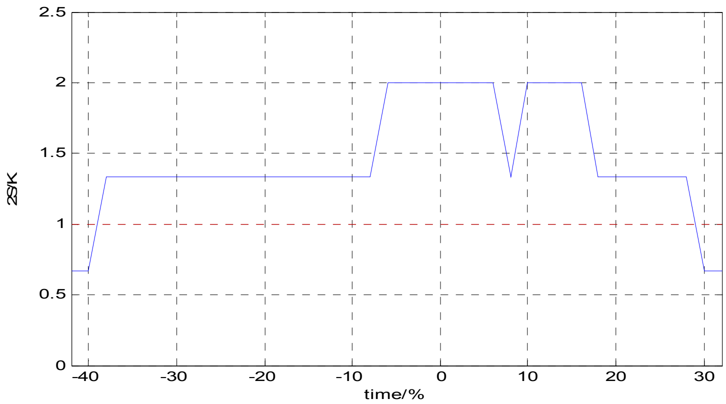

Figure 7. The recognition results of Sequence 7 relative to 6

In the following a group of data from the real test would be used to illustrate that the algorithm possesses the advantages, such as it could reduce some errors in the calculation of RCS which are caused by inaccurate evaluation. The data is composed of point track data and energy information obtained by the signal detection of a radar system. The RCS σ could be derived from the monostatic radar propagation equation given by kerr [19], and it is described as

$$\sigma = (4\pi)^3 P_r R^4 / (P_t G_t G_r \lambda^2 F_t^2 F_r^2) \quad (11)$$

In the equation, P_r and P_t are respectively the power of the received signal and of the transmitted signal, G_r and G_t are the power gain of the receiving antenna and of the transmitting antenna separately; λ is the wavelength, F_t is the propagation factor of the directional diagram from the transmitting antenna to the target, F_r is the propagation factor of the directional diagram from the target to the receiving antenna, and R is the distance from the radar to the target.

The radar equation is performed on real time computation of the RCS of the target, resulting in the RCS sequence needed. A pulse Doppler processing is performed on every 30 pulses, what we got from this forms a point on the sequence of 117 points in total. The target fails to be detected when signal to noise ratio is comparatively low, then velocity super-resolution algorithm would be applied to reconstruct the lost target [20] in order to complement the data. The target is the civil airplane which flies in the speed of 0.26 km/s from about 78 km. The RCS sequences of the airplanes on the same flight, shown as Figure 8 and Figure 9 respectively, are obtained by detecting at different time and recorded as Sequence 8 and Sequence 9.

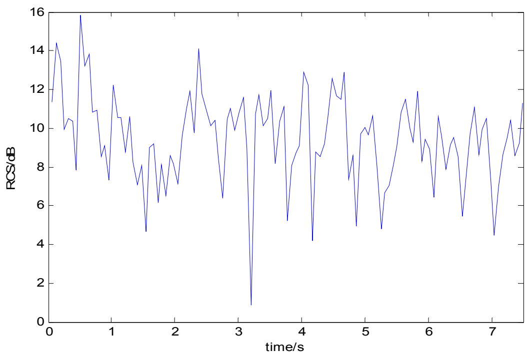

Figure 8. RCS Sequence 8

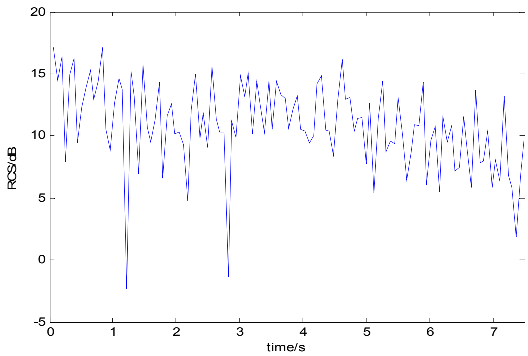

Figure 9. RCS Sequence 9

EMD is performed on these two RCS sequences respectively. Through the results shown as Table 2, the recognition index of the data from the real rest is found to be greater than the previous data. If the total recognition coefficient meets the equation *S*=2, the same target would be still identified.

It is known that the radar equation given by kerr is not comprehensive for not reckoning in some uncertain radar parameters. Therefore, a certain error would exist in the RCS sequences we got. The errors in the computation of RCS caused by these parameters should be a fixed value or at most a fluctuating slowly varying function relative to RCS, which would not significantly affect the normalized instantaneous frequency on high band extracted by EMD. Suppose if the experiment is made under the condition that the other parameters remain the same, and the distance from the radar to the target detected is not precise enough to use, then the data we obtained is only as follows:

$$\sigma / R^4 = (4\pi)^3 P_r / (P_t G_t G_r \lambda^2 F_t^2 F_r^2) \quad (12)$$

Table 2. Data collection of RCS sequences from the real test

IMF	1	2	3	4	5
Instantaneous frequency of Sequence 8	0.6686	0.2674	0.1337	0.0622	0.0267
Instantaneous frequency of Sequence 9	0.6436	0.2348	0.1453	0.0513	0.0256
Energy percentage (%) of Sequence 8	33.12	44.96	8.38	8.52	5.02
Energy percentage (%) of Sequence 9	54.85	28.56	6.61	6.55	3.43
Sequence 9 relative to Sequence 8	R1	R2	R3	S	K/2
	3.74%	12.19%	8.68%	2	1.5

As far as Sequence 8 is concerned, σ / R^4 is seen as a whole, recorded as Sequence 10 after the modification. The algorithm is applied to extract the normalized instantaneous frequency of Sequence 10. Its results are compared with the original data, shown as Table 3. The values of their recognition index, R_1, R_2 and R_3 are very small, and they are in high similarity and could be determined to be the same target. Accordingly, the errors in the calculation of RCS caused by some inaccurate evaluation of slowly varying parameters could be ignored in the algorithm, which would be valuable for the application in engineering practice.

Table 3. Experimental data collection by ignoring the distance *R*

IMF	1	2	3	4	5
Instantaneous frequency of Sequence 8	0.6686	0.2674	0.1337	0.0622	0.0267
Instantaneous frequency of Sequence 10	0.6410	0.2564	0.1282	0.0598	0.0256
Energy percentage (%) of Sequence 8	33.12	44.96	8.38	8.52	5.02
Energy percentage (%) of Sequence 10	33. 76	44. 99	8. 56	8. 05	4. 64
Modification relative to the original sequence	R1	R2	R3	S	K/2
	4.13%	4.11%	4.11%	3	1.5

Finally, in order to verify the effectiveness of the algorithm, three groups of data of Sequence 1, 5 and 8 are compared laterally and the data obtained is collected as Table 4. Shown as Table 4, Sequence 1, 5 and 8 belong to different types of targets, and the recognition index obtained by matching two of them are very great, almost greater than the recognition threshold λ . All S of theirs are all less than $K/2$, so they are recognized as the different targets.

Table 4. Recognition parameters collection of Sequence 1,5 ,and 8

	R1	R2	R3	S	K/2	Same Target？
8 relative to 1	10.29%	30.02%	34.07%	0	1.5	No
5 relative to 1	0.46%	17. 98%	22.73%	1	1.5	No
8 relative to 5	9.88%	14.68%	14.68%	1	1.5	No

7. Conclusion

The paper is the first to propose that EMD is used to analyze RCS time series. The effectiveness and stability of the proposed algorithm are verified by a group of simulated data and two groups of data from the real test. This algorithm could ignore the errors in the calculation of RCS caused by some inaccurate evaluation of slowly varying parameters, which is of great significance to explore the ability of the active narrow-band radar to recognize the target.

References

[1] Nazih NY. *Radar Cross Section of Complex Targets*. Proceedings of the IEEE. 2004; 77(5): 722-734.
[2] Domingo M, Rivas F. Calculation of the RCS Interaction of Edges and Facets. *IEEE Trans. on AP*. 1994; 42(6): 36-47.
[3] Huang Peikang, Yin Hongcheng, Xu Xiaojian, *Radar target characteristics*. Publishing House of Electronics Indestry, Beijing. 2005.
[4] Lin Gang, Xu Jiadong. Study of the Statistical Characterization of Targets′ RCS Dynamic Data. *Modern Radar*. 2006; 28(6): 18-20, 39.
[5] Rao Bin, Qu Longhai, Xiao Shunping, Wang Xuesong. Precession period extraction of ballistic targets based on time series analysis. *Chinese Journal of Radio Science*. 2011; 26(2): 291-296.
[6] Wang Hongyu. *Nonstationary Random Signal Processing and Analysis*. National Defence Industry Press, Beijing. 1999.
[7] Zhang Xianda, Bao Zheng. *Nonstationary Random Signal Processing and Analysis*. National Defence Industry Press, Beijing. 1999.
[8] Huang Xiaohong, Qiu Zhaokun, Chen Zengping, Zhang Zhenzhong. *The Fractal Feature of Space Object RCS*. Chinese Space Science and Technology. 2005; 2(1): 33-36.
[9] Xu Xin, Zhao Anjun, Ji Shashan. Recognition Techniques for Space Targets based on RCS. *Fire Control & Command Control*. 2010; 35(10): 134-136.
[10] Junguo, Zhao Hongzhong, Fu Qiang. Space target recognition algorithm based on RCS sequence. *Aerospace Electronic Warfare*. 2007; 26(6): 14-16.
[11] Tianxu Yang, Jianwei Wang, Xiaoguang Hu. Source: Telkomnika, Research on the mechanical state parameter extraction method of high voltage circuit breakers. *TELKOMNIKA Indonesian Journal of Electrical Engineering*. 2013; 11(5): 2771-2779.
[12] Gupta Manoj, Kumar Rajesh, Gupta Ram Awtar. Neural network based indexing and recognition of power quality disturbances. *TELKOMNIKA Telecommunication Computing Electronics and Control*. 2011; 9(2): 227-236.
[13] Huang NE, Shen Z, Long SR, et al. *The Empirical Mode Decomposition and the Hilbert Spectrum for Nonlinear and Nonstationary Time Series Analysis*. ProcR. Soc. Lond. A. 1998.
[14] Huang NE, Shen Z , Long SR et al. A New View of Nonlinear Water Waves : the Hilbert Spectrum. *Annual Review of Fluid Mechanics*. 1999.
[15] Loutridis SJ. Damage Detection in Gear Systems Using Empirical Mode Decomposition. *Engineering Structures*. 2001; 26: 1833-1841.
[16] Flandrin P, Rilling G, Goncalves P. Empirical Mode Decomposition as a Filter Bank. *IEEE Signal Processing Letters*. 2004; 11: 112-114.
[17] Lin Zhenshan, Wang Shuguang. EMD Analysis of Northern Hemisphere Temperature Variability during Last 4 Centuries. *Journal of Tropical Meteorology*. 2004; 20: 91-96.
[18] He You, Xiu Jianjuan, Zhang Jingwei, Guan Xin. *Radar Data Processing with Applications*. Second ed. Publishing House of Electronics Indestry, Beijing. 2009.
[19] MI Skolnik. *Radar Handbook,Section ed.* Publishing House of Electronics Indestry, Beijing. 2003.
[20] Xia Tian, Shen Yiying, Hou Yuguan, Hou Chengyu. Application of Velocity Super-resolution Algorithm to Lost Target Velocity Spectrum Reconstruction. *11th International Conference on Signal Processing (ICSP'12)*. 2012; 3: 1741-1745.